Eur. Phys. J. A **23**, 191–196 (2005)
DOI 10.1140/epja/i2004-10088-6

THE EUROPEAN PHYSICAL JOURNAL A

Investigation of lifetimes in dipole bands of ^{142}Gd

A.A. Pasternak[1,2], E.O. Podsvirova[1,2], R.M. Lieder[1,a], S. Chmel[3], W. Gast[1], Ts. Venkova[1,4], H.M. Jäger[1], L. Mihailescu[1], G. de Angelis[5], D.R. Napoli[5], A. Gadea[5], D. Bazzacco[6,7], R. Menegazzo[6,7], S. Lunardi[6,7], W. Urban[8], Ch. Droste[8], T. Morek[8], T. Rząca-Urban[8], G. Duchêne[9], and A. Dewald[10]

[1] Institut für Kernphysik, Forschungszentrum Jülich, D-52425 Jülich, Germany
[2] A.F. Ioffe Physical Technical Institute RAS, RU-194021 St. Petersburg, Russia
[3] Institut für Strahlen- und Kernphysik, University of Bonn, D-53115 Bonn, Germany
[4] Institute of Nuclear Research and Nuclear Energy, Bulgarian Academy of Sciences, BG-1784 Sofia, Bulgaria
[5] Istituto Nazionale di Fisica Nucleare, Laboratori Nazionali di Legnaro, I-35020 Legnaro (PD), Italy
[6] Dipartimento di Fisica, Università di Padova, I-35131 Padova, Italy
[7] Istituto Nazionale di Fisica Nucleare, Sezione di Padova, I-35131 Padova, Italy
[8] Institute of Experimental Physics, University of Warsaw, PL-00-681 Warszawa, Poland
[9] Institut de Recherches Subatomique IReS, F-67037 Strasbourg, France
[10] Institut für Kernphysik, Universität zu Köln, D-50937 Köln, Germany

Received: 9 August 2004 / Revised version: 24 September 2004 /
Published online: 7 December 2004 –
Communicated by D. Schwalm

Abstract. Lifetimes have been measured for dipole bands in ^{142}Gd using DSAM. The deduced $B(M1)$ and $B(E2)$ values as well as $B(M1)/B(E2)$ ratios are compared with calculations in the framework of the TAC (Tilted Axis Cranking) and SPAC (Shears mechanism with Principal Axis Cranking) models. The dipole bands DB1 to DB4 can be interpreted as magnetic rotational bands.

PACS. 21.10.-k Properties of nuclei; nuclear energy levels – 21.10.Re Collective levels – 21.10.Tg Lifetimes – 27.60.+j $90 \leq A \leq 149$

1 Introduction

The existence of regular rotational bands, consisting of strong magnetic dipole transitions, in nearly spherical nuclei is well established [1–3]. These bands have been interpreted as resulting from the coupling of the angular momentum vectors $\boldsymbol{j}_1$ and $\boldsymbol{j}_2$ of a few high-j particles of one kind and high-j holes of the other kind of nucleons, respectively, oriented approximately perpendicular to each other at the band head, for generating the total spin of the nucleus [3]. This coupling results in a substantial component of the magnetic dipole moment which is transverse to the total spin. As this component of the magnetic dipole moment rotates around the vector of the total angular momentum, this new mode has been called "Magnetic Rotation" (MR) [3]. The angular momentum of the band is increased by the gradual alignment of the individual nucleon spins along the total-angular-momentum vector. This way of angular-momentum production has been called "shears mechanism". The MR bands have very large $B(M1)$ values (several μ_N^2) and their crossover transitions, if existent at all, have very small $B(E2)$ values ($\approx 0.1(eb)^2$). Because of the alignment of the nucleons the $B(M1)$ values are decreasing with increasing spin.

Magnetic rotations are expected in regions close to magic numbers if high-j nucleons are available and the deformation is small [3]. Also for the $N \approx 82$ region MR bands are predicted and four dipole bands have been found in ^{142}Gd [4] which were considered as MR bands from a comparison of the frequency dependence of their angular momenta I and their ratios of reduced transition probabilities $B(M1)/B(E2)$ with predictions of the Tilted Axis Cranking (TAC) model [3]. The dipole bands DB1 and DB2 in ^{142}Gd are considered to have $\pi h_{11/2}^2 \otimes \nu h_{11/2}^{-2}$ and $\pi h_{11/2}^2 \otimes \nu h_{11/2}^{-4}$ and DB3 and DB4 $\pi h_{11/2}^1 \otimes \pi g_{7/2}^{-1} \nu h_{11/2}^{-2}$ and $\pi h_{11/2}^1 \otimes \pi g_{7/2}^{-1} \nu h_{11/2}^{-4}$ configurations, respectively [4]. In the present work a further dipole band, denoted DB5, has been found. A proof for the interpretation of the dipole bands in ^{142}Gd as MR bands may result from lifetime measurements and the determination of $B(M1)$ and $B(E2)$ values. A preliminary report on the present investigation can be found in ref. [5]

[a] e-mail: r.lieder@fz-juelich.de

2 Experimental methods and results

With EUROBALL IV at IReS Strasbourg a lifetime experiment using the Doppler-shift attenuation method (DSAM) has been carried out which allowed to determine the $B(M1)$ and $B(E2)$ values of the dipole bands DB1 to DB4 in ^{142}Gd. To minimize the sidefeeding lifetimes, a ^{114}Sn(^{32}S, 2p2n) reaction at a beam energy of 160 MeV has been used. As target a self-supporting metallic ^{114}Sn foil of 8 mg/cm^2 thickness with an enrichment of 71.1% has been used. The initial recoil velocity is $v/c = 2.2\%$ for this reaction. EUROBALL IV (consisting of 14 CLUSTER, 26 CLOVER and 30 individual Compton-suppressed Ge detectors) was equipped with an inner BGO ball and the particle detector array EUCLIDES. Events were recorded when ≥ 5 unsuppressed Ge detectors fired in coincidence. Approximately $4.3 \cdot 10^9$ high-fold γ-events have been collected. The energy and efficiency calibrations of the EUROBALL IV array have been carried out with a ^{152}Eu source.

To extract lifetimes the data have been sorted into several γ-γ-γ-cubes for which the γ-ray energies from any detector were stored into the first two axes and the energies from detectors placed under a certain angle with respect to the beam direction in the third axis of the respective cube. The DSAM line shape analysis was hence carried out in doubly-gated coincidence spectra. The detector rings at average angles of 133° (10 CLUSTER detectors), 103° (13 CLOVER detectors) and 77° (13 CLOVER detectors) have been used, because the corresponding spectra have the highest statistics. These cubes contain $54 \cdot 10^9$, $54 \cdot 10^9$ and $59 \cdot 10^9$ γ-γ-γ-events, respectively. The energy and time calibrations, the presort and the sort of the γ-γ-γ-cubes has been carried out with the software package *Ana* [6]. Since the instrumental lineshapes and efficiencies of the various detector rings differ from each other they have been determined separately for each ring.

The analysis of experimental DSAM lineshapes was carried out using updated versions of the Monte Carlo codes COMPA, GAMMA and SHAPE [7]. The "wide gate below" technique has been applied to obtain sufficient statistics in the analysed spectra. Therefore, side feeding has to be taken into account. The side-feeding cascades between the entry states of the final nucleus and the considered levels have been simulated taking into account statistical $E1$, $M1$ and $E2$ transitions and stretched $E2$ bands with rotational damping. Because ^{142}Gd is situated close to the semi–doubly-magic nucleus ^{146}Gd, furthermore, the influence of superdeformed bands and the existence of a large amount of particle-hole excitations in the entry-state region, which generate bands of magnetic dipole transitions, are considered [7]. The time distributions of the side feeding have been calculated with Monte Carlo methods and the relevant parameters were determined by the investigation of γ-ray multiplicity spectra for $^{142-146}$Gd [8]. For the 790 keV $20^+ \rightarrow 18^+$ transition of the $(+,0)_1$ band of ^{142}Gd [4] the side-feeding calculations could be checked since it is sufficiently intense and the 20^+ level has an appropriate lifetime. For this line the lifetime analysis was carried out for spectra obtained by the "wide gate below" technique and by gating from above on the flight component of the peak. The deduced lifetimes of 0.68 ± 0.06 and $0.71^{+0.17}_{-0.11}$ ps, respectively, agree well indicating that the side-feeding calculations are correct. The effective sidefeeding lifetime of the 17^+ level in the dipole band DB1 is $\tau_{\rm eff} \approx 0.25$ ps and decreases with increasing spin. In some cases the spectra for the symmetric angles of 77° and 103° have been added to improve the statistics. The resulting DSAM lineshapes are then symmetric. The uncertainties result from statistical contributions and from uncertainties related to the cascade- and side-feeding pattern as well as from the uncertainty of the stopping power for the recoils. The statistical uncertainties are obtained by a χ^2 analysis taking into account the variable parameters of all peaks in the fitted multiplet. Intensities, important for taking into account cascade feeding, have been evaluated from the fit of the DSAM lineshapes in the spectra. They are consistent with the intensities obtained in the previous experiment [4].

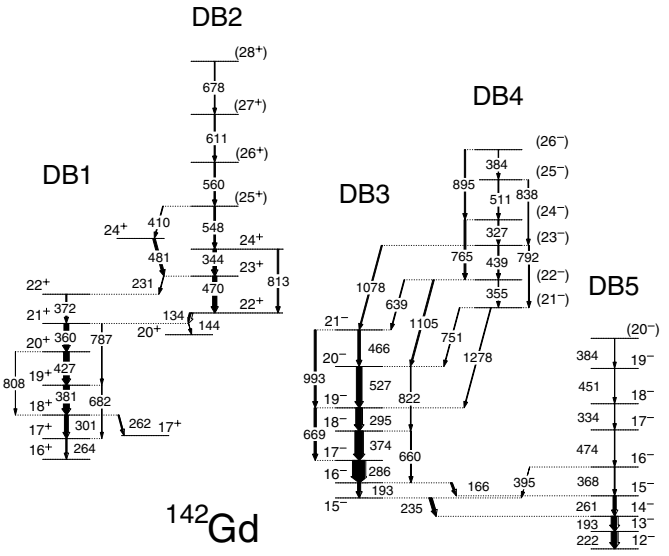

Fig. 1. Partial level scheme showing the dipole bands of ^{142}Gd. The widths of the arrows represent the relative intensities of the transitions.

The investigated dipole bands of ^{142}Gd are shown in fig. 1. With respect to our previous work [4] the dipole band DB5 has been added. It was found in a re-analysis of the EUROBALL III experiment in which ^{142}Gd was produced in the ^{99}Ru(^{48}Ti, 2p3n) reaction at 240 MeV [4]. The low-spin members of dipole band DB5 were already known, since they are populated in the de-excitation of DB3, but the order of the 193 and 235 keV lines in the $16^- \rightarrow 15^- \rightarrow 14^-$ sequence has been exchanged with respect to our previous work [4]. Angular-distribution ratios [4] have been used to determine the mutlipole orders of the 334, 368, 395, 451 and 474 keV transitions in DB5. They range from $R_{\rm AD} = 0.4$ to 0.6 as expected for $\Delta I = 1$ transitions and have $E2/M1$ mixing paramters of $\delta = -0.2 \pm 0.1$. The dipole band DB5 is for $I \geq 16$ about 20 times weaker populated than DB3.

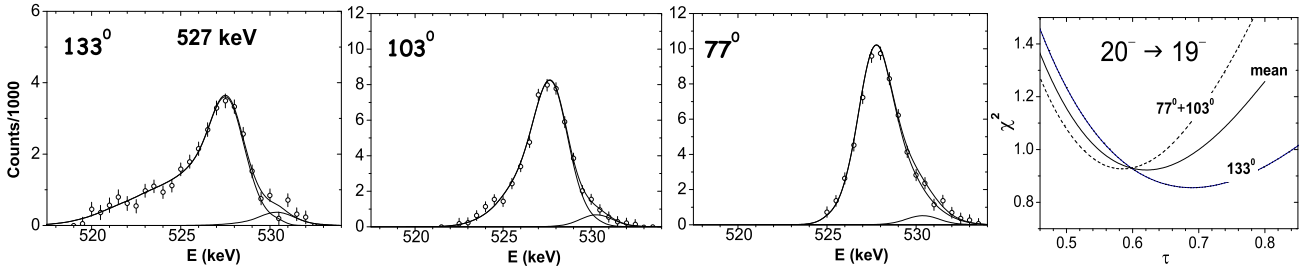

Fig. 2. Lineshape analysis for the 527 keV $20^- \rightarrow 19^-$ transition of DB3 in ^{142}Gd. The lifetimes have been obtained in a χ^2 analysis. The avarage value with its statistical uncertainty is $\tau = 0.62 \pm 0.13$ ps.

Table 1. Lifetimes and $B(M1)$ and $B(E2)$ values resulting from the lifetimes and transition intensities as well as $\frac{B(M1)}{B(E2)}$ ratios deduced from branching ratios for the dipole bands DB1 to DB4 of ^{142}Gd.

I_i^π	τ (ps)	$B(M1)$ (μ_N^2)	$B(E2)$ (10^{-2} e^2b^2)	$\frac{B(M1)}{B(E2)}$ $(\mu_N/eb)^2$
17^+	$2.2^{+0.8}_{-0.5}$	$0.19^{+0.11}_{-0.04}$		
18^+	$1.3^{+0.4}_{-0.3}$	$0.71^{+0.37}_{-0.14}$ $0.49^{+0.28}_{-0.09}$ (a)		
19^+	$0.54^{+0.25}_{-0.15}$	$1.29^{+0.95}_{-0.25}$	$1.7^{+1.9}_{-0.7}$	56^{+83}_{-8}
20^+	$0.52^{+0.20}_{-0.15}$	$1.10^{+0.77}_{-0.20}$	$1.8^{+1.6}_{-0.5}$	53^{+25}_{-8}
21^+	$0.94^{+0.21}_{-0.16}$	$1.04^{+0.38}_{-0.18}$ $0.48^{+0.38}_{-0.21}$ (a)	$1.7^{+0.9}_{-0.4}$	55^{+20}_{-9}
22^+	$0.98^{+0.40}_{-0.25}$	$0.91^{+0.58}_{-0.17}$		
23^+	0.33 ± 0.11	$1.22^{+1.00}_{-0.20}$ $1.64^{+1.46}_{-0.29}$ (a)		
24^+	0.64 ± 0.15	$1.38^{+0.69}_{-0.24}$	$10.1^{+5.4}_{-1.9}$	$13.3^{+3.1}_{-2.1}$
25^+	0.35 ± 0.15	$0.56^{+0.69}_{-0.10}$ $0.51^{+0.78}_{-0.11}$ (a)		
26^+	0.27 ± 0.15	$0.86^{+1.55}_{-0.12}$		
17^-	1.3 ± 0.5	$1.48^{+1.56}_{-0.24}$		
18^-	1.1 ± 0.3	$0.79^{+0.47}_{-0.13}$	$5.8^{+3.8}_{-1.1}$	$13.1^{+2.7}_{-1.4}$
19^-	$1.6^{+0.5}_{-0.3}$	$0.87^{+0.37}_{-0.17}$	$8.8^{+3.9}_{-1.6}$	$9.7^{+1.2}_{-0.8}$
20^-	0.62 ± 0.13	$0.53^{+0.22}_{-0.08}$	$3.5^{+1.8}_{-0.8}$	$14.0^{+5.2}_{-1.8}$
21^-	$0.71^{+0.17}_{-0.15}$	$0.40^{+0.18}_{-0.07}$	$4.8^{+2.3}_{-0.9}$	$8.1^{+1.5}_{-1.1}$
22^-	$0.44^{+0.20}_{-0.18}$	$0.46^{+0.55}_{-0.08}$		
23^-	$0.77^{+0.25}_{-0.20}$	$0.25^{+0.17}_{-0.05}$	$9.1^{+6.4}_{-2.9}$	$2.2^{+2.3}_{-0.4}$
24^-	$1.2^{+0.4}_{-0.3}$	$0.40^{+0.30}_{-0.10}$	$14.4^{+9.5}_{-2.9}$	$2.6^{+1.4}_{-0.7}$
25^-				$2.3^{+1.6}_{-0.6}$
26^-				$2.3^{+1.6}_{-0.7}$

(a) $B(M1)$ value of the second dipole transition, depopulating the level out of the band.

Lifetimes have been deduced for 18 levels of the dipole bands DB1 to DB4 in ^{142}Gd. The DSAM lineshape analysis for the 527 keV $20^- \rightarrow 19^-$ transition of DB3 is shown in fig. 2. The spectra result from the 133° CLUSTER detector as well as 77° and 103° CLOVER detector rings and were obtained by summing various clean gate combinations of transitions lying below the 19^- level to enhance the statistics. The lifetimes and the deduced $B(M1)$, $B(E2)$ and $B(M1)/B(E2)$ values are given in table 1. The $B(M1)$, $B(E2)$ and $B(M1)/B(E2)$ values and their uncertainties have been calculated with Monte Carlo methods since the errors of the lifetimes and intensities are large and the application of the error propagation law underestimates the uncertainties. In the Monte Carlo simulations the probability distributions for the resulting quantities have been calculated assuming Gaussian probability distributions for the lifetimes and intensities. The resulting probability distributions are not any more Gaussian and the most probable $B(M1)$, $B(E2)$ and $B(M1)/B(E2)$ values, respectively, are taken with uncertainties reflecting a 68% confidence interval. The most probable values deviate from the median values which equal the values obtained using the well-known equations for these quantities [9].

3 Discussion

Calculations have been carried out in the framework of the TAC model [3] and a semi-classical model similar to the Clark and Macchiavelli approach [2]. In this semiclassical description originally the case was considered that the total spin is produced solely by the shears effect and the collective rotation is absent. Then only the angle between the angular momentum vectors of the involved particles and holes $\boldsymbol{j}_1$ and $\boldsymbol{j}_2$ is of importance [2]. Collective rotation has been added to this model [11] in the framework of a coupling scheme, in which the vectors $\boldsymbol{R}$ and $\boldsymbol{j} = \boldsymbol{j}_1 + \boldsymbol{j}_2$ are parallel to each other.

In the present work another approach has been chosen in which the shears mechanism is combined with the Principal Axis Cranking (PAC) coupling scheme [10], in which the angular-momentum vector $\boldsymbol{R}$ of the collective rotation is parallel to the x-axis. This semiclassical model has been called "Shears mechanism with Principal Axis Cranking" (SPAC) model and is described in more detail in refs. [5,9]. In the SPAC model the total energy is given

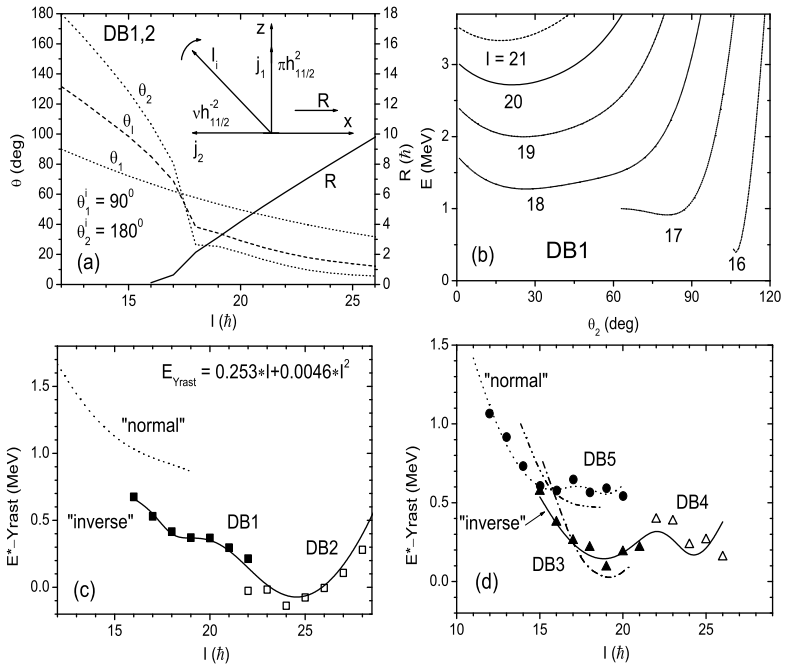

Fig. 3. (a): Evolution of the angles θ_1, θ_2, θ_I and the rotational angular momentum R with spin for the "inverse" initial alignment for the dipole bands DB1 and DB2 in ^{142}Gd. (b) Total energy as function of the angle θ_2 for DB1. (c) Comparison of the calculated spin dependence of the level energy for DB1 and DB2 for the normal and inverse initial alignments with experimental results. (d) Same as (c) for DB3 to DB5. For DB3 and DB5 also results of TAC model calculations are shown as dash-dot and dash-dot-dot lines, respectively.

by $E(I,\theta_1,\theta_2) = 1/(2J)\ R^2(I,\theta_1,\theta_2) + V_2\ P_2(\theta_1-\theta_2) +$ const, where $P_2(\theta_1-\theta_2) = [3\cos^2(\theta_1-\theta_2)-1]/2$ and $R(I,\theta_1,\theta_2) = \sqrt{I^2-(j_1\sin\theta_1+j_2\sin\theta_2)^2} - j_2\cos\theta_2 - j_1\cos\theta_1$. Generally, any initial orientation of the angular-momentum vectors $\boldsymbol{j}_1$ and $\boldsymbol{j}_2$ can be considered. The two symmetric initial orientations of $\boldsymbol{j}_2$, resulting from a rotation by $\Re_z(\pi)$, while the initial orientation of $\boldsymbol{j}_1$ remains unchanged, have been called "normal" and "inverse" initial alignments. They can generate three different dipole bands considering that $\boldsymbol{j}_1$ and $\boldsymbol{j}_2$ can in the inverse case move in such a way that for a certain total angular momentum they are oriented parallel or antiparallel to each other. The vector coupling scheme for the "inverse" initial alignment is depicted in the inset of fig. 3a. The angles of the angular-momentum vectors $\boldsymbol{j}_1$ and $\boldsymbol{j}_2$ with respect to the rotation axis are θ_1 and θ_2, respectively. The evolution of the angles θ_1, θ_2 and θ_I, representing the orientation of the total angular momentum $\boldsymbol{I} = \boldsymbol{j}_1 + \boldsymbol{j}_2 + \boldsymbol{R}$ with respect to the rotation axis, as a function of spin are shown in fig. 3a for the inverse initial alignment. For θ_1 the spin dependence is described as $\theta_1(I) = \theta_1^i\ \exp[(1-I/I_i)\alpha]$, with $\alpha = 0.9$. This spin dependence has been assumed, considering that the vector $\boldsymbol{j}_1$ should initially have $\theta_1^i = 90°$ and becomes fully aligned at high spins ($\theta_1 = 0°$). The parameter α decribes how rapidly full alignment is achieved. The angle θ_2 and the level energies are found by a minimization of the total energy using the condition $(\frac{\mathrm{d}E}{\mathrm{d}\theta_2})_I = 0$. The energy as a function of θ_2, shown for the dipole band DB1 in fig. 3b from $I = 16$, has been calculated considering the $\pi h^2_{11/2} \otimes \nu h^{-2}_{11/2}$ configuration (cf. sect. 1). For smaller spins no solution has been found for the above-described choice of parameters in agreement with the fact that this band is observed only from $I = 16$ (cf. fig. 1). The angle θ_2 and the level energies are taken from the respective energy minima. For DB3 similar calculations have been carried out considering a $\pi h^1_{11/2} \otimes \pi g^{-1}_{7/2} \nu h^{-2}_{11/2}$ configuration. It was found that no solution exists for $I < 15$ in agreement with the experimental observation (cf. fig. 1).

The calculated spin dependence of the level energy is compared with the experimental one for DB1 and DB2 in fig. 3c for the normal and inverse initial alignments. It can be seen that the inverse initial alignment is energetically favoured as compared to the normal one and that it can explain the data very well. A similar comparison for the dipole bands DB3 to DB5 is shown in fig. 3d. It can be seen that DB3 and DB4 correspond to the inverse and DB5 to the normal initial alignment.

In fig. 4 the experimental results for the dipole bands DB1 to DB5 in ^{142}Gd are compared with calculations in the framework of the TAC and SPAC models. In this figure the angular momentum I is plotted *vs.* the rotational frequency $\hbar\omega$ (fig. 4a) whereas the $B(M1)$ (fig. 4b) and $B(E2)$ (fig. 4c) values as well as the $B(M1)/B(E2)$ ratios (fig. 4d) are plotted as a function of spin. The latter three values have been taken from table 1. The 18^+ and 21^+ levels of DB1 as well as the 23^+ and 25^+ levels of DB2 are depopulated, however, by two dipole transitions each (cf. fig. 1). For these cases the $B(M1)$ values shown in fig. 4b

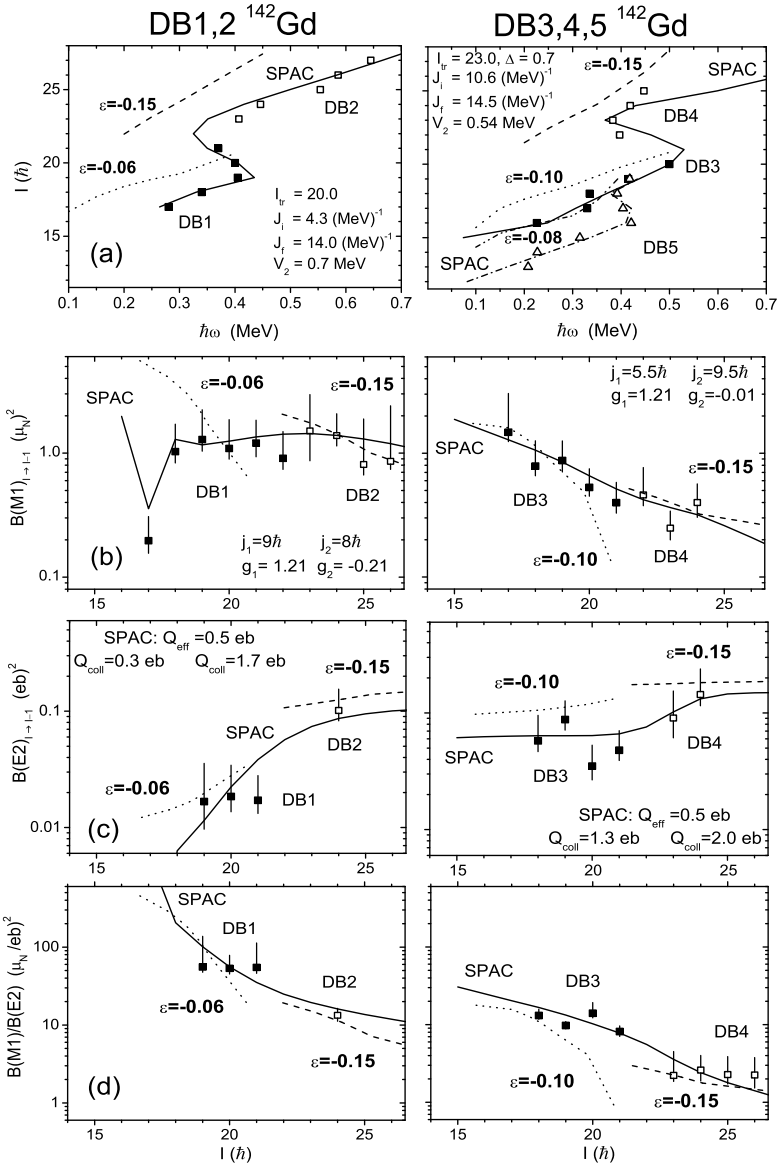

Fig. 4. Comparison of experimental results for the dipole bands DB1 to DB5 in ^{142}Gd with those of calculations in the framework of the TAC and SPAC models: (a) angular momentum I *vs.* rotational frequency $\hbar\omega$, (b) $B(M1)$ values, (c) $B(E2)$ values, (d) $B(M1)/B(E2)$ ratios. The TAC calculations are shown as dotted lines for DB1 and DB3, as dashed lines for DB2 and DB4 and as dash-dot-dot line for DB5. The used deformations are given. The SPAC results for the inverse and normal initial alignments are shown as full (DB1 to DB4) and dash-dotted (DB5) lines, respectively.

were calculated by taking the average of the values for the band members and the sum of the values for both dipole transitions.

Results of the SPAC model calculations for DB1 to DB4 in ^{142}Gd for the inverse initial alignment are shown as full lines in fig. 4. The above-mentioned configurations have been assumed for DB1 and DB3. At the spin $I_{\rm tr} = 20$ for DB1 and 23 for DB3 an increase of the collective transitional quadrupole moment $Q_{\rm coll}$ [9] and the moment of inertia $\mathcal{J}$ is assumed (cf. figs. 4a,c) which allows to explain the backbending between DB1 and DB2 as well as DB3 and DB4, respectively, seen in fig. 4a. This implies a structural change of the core. For DB1 and DB2 the difference between the collective quadrupole moments $Q_{\rm coll}$ obtained in the SPAC model calculations is much larger than reflected by the difference in deformations obtained in the TAC model (see below). This can be explained, considering that both $Q_{\rm coll}$ and the quasiparticle transitional quadrupole moment $Q_{\rm eff}$ contribute to the $B(E2)$ values [9]. It should be pointed out that the small $B(M1)$ value found for the 17^+ level of DB1 can be reproduced by the SPAC model calculations. This is a feature of the inverse initial alignment scheme since, as can be seen in fig. 3a, θ_1 and θ_2 become equal close to this spin which means that $\boldsymbol{j}_1$ and $\boldsymbol{j}_2$ assume a parallel orientation and the transverse component of the magnetic dipole moment

rotating around the vector of the total angular momentum vanishes at the crossing point. The SPAC model can very well reproduce the measured quantities with a considerable contribution of collectivity. For dipole band DB5 the aligned angular momentum as a function of the rotational frequency can be reproduced by SPAC calculations assuming normal initial alignment as shown by a dash-dotted line in fig. 4a. The same configuration as for DB3 is considered.

The TAC model calculations for ^{142}Gd [4] are shown as dotted and dashed curves in fig. 4. They are based on the four and six particle-hole configurations mentioned in the introduction section for DB1/DB3 and DB2/DB4. The results of the TAC model calculations for DB1 and DB2 using deformations of $\varepsilon_2 = -0.06$ and -0.15 ($\varepsilon_4 = 0$ and $\gamma = 0$), respectively, are shown in fig. 4. It is expected that the alignment of a second $\nu h_{11/2}$ hole pair causes an increase of the deformation suggesting that the deformation for DB2 is larger than for DB1. For DB1 the deformation has been decreased with respect to the value of $\varepsilon_2 = -0.10$ used in ref. [4], to reproduce the experimental $B(E2)$ values. This improves also the $B(M1)/B(E2)$ ratios of DB1 with respect to the previous publication [4]. For DB3 and DB4 results of the TAC model calculations are shown in fig. 4 for $\varepsilon_2 = -0.10$ and -0.15, respectively. Considering all plotted quantities, the TAC model calculations can quite well reproduce the experimental results. For DB5 TAC model calculations have been carried out for a $\pi h^1_{11/2} \otimes \pi d^{-1}_{5/2} \nu h^{-2}_{11/2}$ configuration at a deformation $\varepsilon_2 = -0.08$ which can reproduce the frequency dependence of the aligned angular momentum reasonably well. The difference of excitation energies between DB3 and DB5 could be extracted from the TAC model calculations since the same set of parameters has been used for both bands. The TAC model results can reproduce well the experimental values as can be seen in fig. 3d.

The dipole bands DB1 and DB2 in ^{141}Eu were considered to result from the configurations of DB1 and DB2 in ^{142}Gd by subtraction of one $h_{11/2}$ proton [9]. The deformation parameters of the TAC model calculations for ^{141}Eu were $\varepsilon_2 = -0.07$ and -0.09, respectively, for DB1 and DB2. The deformations for DB1 in ^{141}Eu and ^{142}Gd are similar because the $B(E2)$ value and the tilting angle are for ^{141}Eu larger than for ^{142}Gd. The tilting angles, which enter as $\sin^4\theta$ in the calculation of the $B(E2)$ value, are different for these two nuclei because of the different lengths of the shears blades. For DB2 the $B(E2)$ values are similar for these two nuclei so that the difference in the deformation parameters reflect the difference in the tilting angles.

The comparison of the experimental results with those of the TAC and SPAC models indicate that the dipole bands in ^{142}Gd can indeed be considered as magnetic rotational bands.

4 Summary

Lifetimes have been measured for the dipole bands in ^{142}Gd using DSAM with EUROBALL IV employing the ^{114}Sn(^{32}S, 3p2n) reaction at a beam energy of 160 MeV. Lifetimes have been determined for 18 levels of the dipole bands DB1 to DB4. The deduced $B(M1)$ and $B(E2)$ values as well as $B(M1)/B(E2)$ ratios are well described by calculations in the framework of the TAC (Tilted Axis Cranking) and SPAC (Shears mechanism with Principal Axis Cranking) models. The dipole bands can be interpreted as magnetic rotational bands.

A new dipole band (DB5) has been found by a reanalysis of the EUROBALL III experiment in which ^{142}Gd was produced in a ^{99}Ru(^{48}Ti, 2p3n) reaction at 240 MeV. The dipole bands DB3 and DB5 are considered in the SPAC model as resulting from the $\pi h^1_{11/2} \otimes \pi g^{-1}_{7/2} \nu h^{-2}_{11/2}$ configuration of inverse and normal initial alignment, respectively. In the TAC model a $\pi h^1_{11/2} \otimes \pi d^{-1}_{5/2} \nu h^{-2}_{11/2}$ configuration has been considered for DB5. More experimental information is needed to distinguish between the two configuration assignments.

We are grateful to the accelerator crew in Strasbourg for providing the beam and to the EUROBALL crew for technical support. The work was partly supported by IB of BMBF at DLR, Germany under the WTZ contract RUS 99/191, by the Heinrich Hertz Foundation, Germany under the contract No. 16/03 and by the EU under the TMR contract ERBFMRXCT970123 and the LSF contract HPRI-CT-1999-00078. Enlightening discussions with S. Frauendorf and H. Hübel on the SPAC model are gratefully acknowledged.

References

1. H. Hübel *et al.*, Z. Phys. A **358**, 237 (1997).
2. R.M. Clark, A.O. Macchiavelli, Annu. Rev. Nucl. Part. Sci. **50**, 36 (2000).
3. S. Frauendorf, Rev. Mod. Phys. **73**, 463 (2001).
4. R.M. Lieder *et al.*, Eur. Phys. J. A **13**, 297 (2002).
5. R.M. Lieder *et al.*, *Proceedings of the International Conference on The Labyrinth in Nuclear Structure, Crete, Greece*, edited by A. Bracco, C.A. Kalfas, AIP Conf. Proc. **701**, 238 (2004).
6. W. Urban, Manchester University, Nuclear Physics Report 1991-1992, p. 95.
7. R.M. Lieder *et al.*, Eur. Phys. J. A **21**, 37 (2004).
8. A.A. Pasternak *et al.*, Laboratori Nazionali di Legnaro Annu. Rep. 2001, p. 44 and 2002, p. 17 web edition: `www.lnl.infn.it`; *Investigation of fold distributions for residual nuclei produced in the $^{114}Cd + ^{36}S$, $^{100}Mo + ^{48}Ti$ and $^{97}Mo + ^{51}V$ reactions,* to be submitted to Eur. Phys. J. A.
9. E.O. Podsvirova *et al.*, Eur. Phys. J. A **21**, 1 (2004).
10. F. Dönau, S. Frauendorf, *Proceedings of the Conference on High Angular Momentum Properties of Nuclei, Oak Ridge 1982*, edited by N.R. Johnson, Nucl. Sci. Res. Conf. Ser. **V4** (Harwood, New York, 1983) p. 143.
11. A.O. Macchiavelli *et al.*, Phys. Lett. B **450**, 1 (1999).